

Microfluidic arrangement with an integrated micro-spot array for the characterization of pH and solvent polarity

A.R. Thete^{a,*}, G.A. Gross^a, T. Henkel^b, J.M. Koehler^{a,b}

^a Technical University of Ilmenau, Institute for Micro and Nano Technologies, Department of Microreaction Technology, Weimarerstr. 32, D-98693 Ilmenau, Germany

^b Institute for Physical High Technology, Albert-Einstein-Str. 9, 07745 Jena, Germany

Abstract

Micro-spot arrays with different pH and polarity sensitive fluorescence dyes were prepared using a piezo dispensing head. A polyethylene glycol matrix was used to immobilize the dyes covalently. The polymer matrix was cross-linked to ensure stable dye bonding and for controlling the swelling and permeability of the thin film. Analytical experiments were carried out in the fluidic phase with specially developed micro-fluidic and CCD imaging optical set-up. As a result, different solvents and solutions could be distinguished for their pH and polarity using fluorescence digital imaging. After calibration, a quantitative determination of the solution composition was also possible. The chemo-chips were tested against different solvent species leading to confirmation of the applicability of the developed spot array for the reproducible recognition of different liquid types focusing on polarity and pH as parameters.

© 2007 Elsevier B.V. All rights reserved.

Keywords: Chemo-chips; Array technique; Chemical recognition; Fluorescence digital imaging; Multi-component analysis; Pattern recognition

1. Introduction

Recently, array technology has been extensively used in the field of biotechnology for gene expression studies more commonly known as DNA chips, protein chips, and carbohydrate chips [1]. These techniques make use of the specific interaction between the probe molecule embedded in the spot array and the analyte molecular sequence. Analogously for the ‘chemo-chip’ approach, a micro-spot array of solvatochromic dyes and pH indicator dyes [2–6] is built for short-term determination of the polarity of solvent mixtures and online pH determination, which is of great interest in chemical synthesis [7–10]. In principle, chemo-chip efforts are focused on developing a universal tool for the recognition of general chemical species in fluidic phases. It is next to impossible to have the perfect universal chip as a sensor for the enormous number of chemical species with specific probe–analyte interactions such as covalent binding, complex formation, hybridisation, and hydrogen bonding, which is the case for biochips [11,12]. There has been a lot of work done on the electronic nose for detection of analytes in the gaseous phase using specific as well as non-specific

interactions [13–16]. These techniques are also applied in the characterization of complex composed liquids like coffee, beer, and wine as well as in special diagnostics like human breath analysis [17–21]. Therefore, to widen the span of chemo-chip detection of chemical liquids as much as possible, we have adopted the approach of non-specific interactions only. In doing so, the special high performance digital imaging technique for fluorescence measurements proves to be a more powerful and sensitive tool when compared to the other optical techniques like colorimetry or conventional optical spectroscopy. The optical signal generated by a digital imaging technique has been processed, to obtain an empirically generated fluorescence pattern depending on the fluorescence quenching or enhancing interaction of the various dyes present in the micro-array. This strategy gives the potential of developing an advance pattern recognition system if employed on multi-component cross-reactive arrays [22]. Development of fluorescent spot arrays for chemical sensor application requires knowledge about the influence of solvent polarity on the fluorescence behavior of each sensor spot. In order to optimize each dye spot in the micro-array, we have investigated the solvatochromic fluorescence behavior [23,24] of different spot types simultaneously, under the influence of series of solvent mixtures with varying polarity (Fig. 1). The numbered E_N^T empirical polarity unit has been used for the clas-

* Corresponding author. Tel.: +49 3677 69 3437.

E-mail address: aniket.thete@tu-ilmenau.de (A.R. Thete).

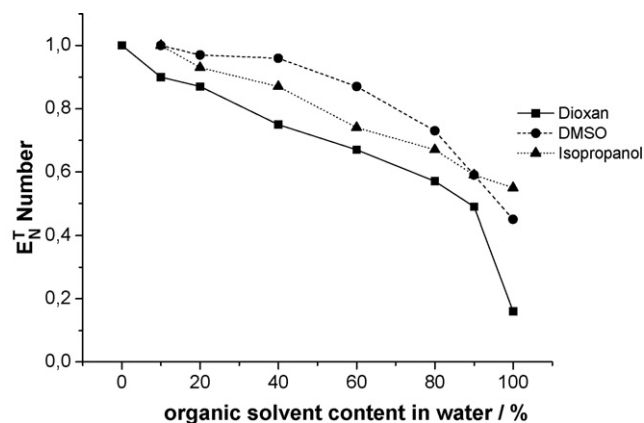


Fig. 1. Polarity of the analyte sample expressed in E_N^T number empirical units as a function of organic solvent content in water. The values are calculated from absorption λ_{\max} measurements of Reichardt's betaine dye.

sification of polarity of the analyte samples discussed here [25]. Hence, the determination of a set of general chemical properties can be applied together with selected indicator functions. Polyethylene glycol films coated on glass (IPHT, Jena) have been used as an immobilization substrate. The experimental set-up consists of an optical bench with visible light source, CCD digital imaging camera set, optical filters, mirrors, lenses, and an integrated micro-fluidic arrangement. Here, the development of a chemo-chip based on the micro-spot array technology, the construction of a micro-fluidic set-up for reproducible analytical application, and the testing of results on different liquid analytes are reported.

2. Experimental

2.1. Composition and preparation of micro-spots

In our study, four fluorescent dyes were used. These are mainly polarity sensitive solvatochromic dyes, namely 5-

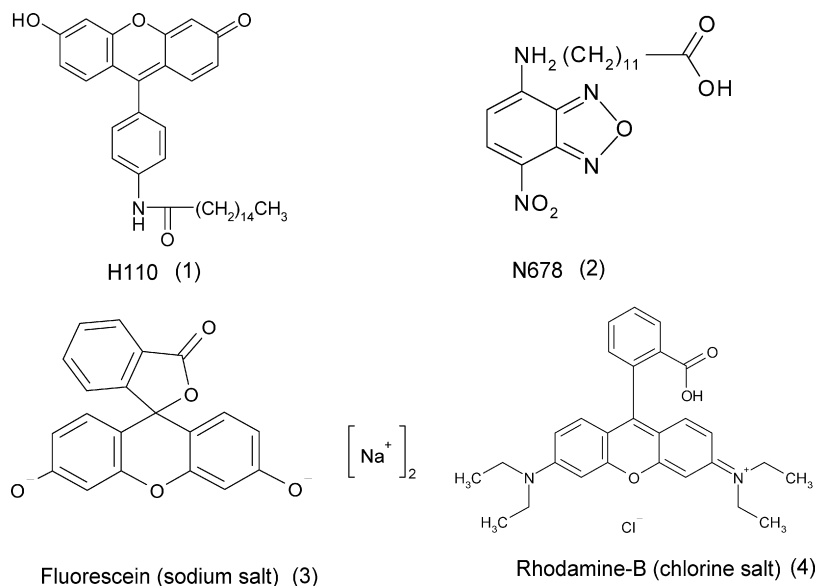


Fig. 2. Indicator dyes used as probes in the micro-spot array.

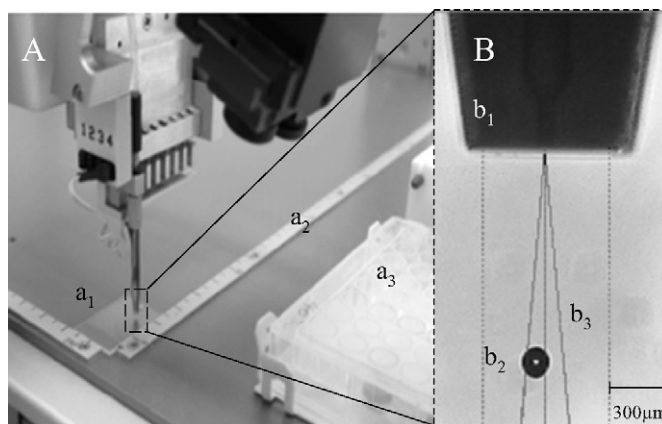


Fig. 3. (A) Scripting dye spot array on a polymer film using a Nanoplotter (GeSim mbH): (a₁) polymer film coated glass chip; (a₂) X–Y plotter scale; (a₃) micro-titre plate. (B) (b₁) Stroboscopic image at a speed of 250 $\mu\text{s}/\text{frame}$ of the nano-dispensing head with spot adjustment scales; (b₂) dye solution droplet; (b₃) margin for spot positioning.

hexadecanoylamino fluorescein (1) (H110, Invitrogen Inc.) and 12-(*N*-(7-nitrobenz-2-oxa-1,3-diazol-4-yl)amino)dodecanoic acid (2) (N678, Invitrogen Inc.) and the pH sensitive dyes Fluorescein (3) and Rhodamine-B (4) (Fig. 2). These dyes were bound covalently to a polymer using *N*-ethyl-*N'*-(3-dimethylaminopropyl) carbodiimide hydrochloride (EDCI) as coupling reagent which forms an ester linkage using the carboxylic acid group on the dye molecule and the hydroxyl group from the polymer itself. 4-Di(methylamino)pyridine (DMAP) and *N*-ethyldiisopropylamine solution (DIPEA) were used as catalyst and base, respectively.

The solution of dyes and coupling reagents were prepared in dimethyl formamide (DMF). These solutions were then loaded into the Nanoplotter (GeSim mbH) device, which spotted these solutions to form a micro-spot array. The Nanoplotter (Fig. 3) consists of a nano-dispensing silicon tip bearing a photolithographically created micro-channel covered with glass. This

dispensing head can deliver a droplet of ~ 350 nL minimum volume with the help of a piezo block fitted on the rear side of the dispensing tip. The spot volume can be controlled by changing the voltage, frequency or pulse width of the piezo which creates a rectangular pulse. The pulses are transferred to the liquid present in the micro-channel. As a result of this, a drop is given out from the tip. A diagonal spotting pattern was adopted to spread the spots all over the array yet maintain simplicity of array design for further image analysis. The complete loading and unloading of solutions in the piezo tip and the spotting procedure was programmed. A batch of 20 chips for array spotting can be carried out for better reproducibility of spot arrays.

After spotting the dye-coupling solution, the chips were heated to 40°C for 10 min on a hot plate to carry out the coupling reaction. Subsequently, they were washed with DMF and water to remove the excess unbound dye from the polymer matrix.

The reversibility of such a chip depends on the nature of analyte liquid interacting with the matrix and the reversibility of the fluorescence change. The spot size was estimated to be $\sim 100\ \mu\text{m}$ with a spacing of $75\text{--}100\ \mu\text{m}$ depending on the wetting ability of different dye solutions on the polymer surface. The positioning of spots is critically dependent on the conditions of droplet formation from the nano-tip and is monitored and controlled using a stroboscope imaging camera integrated in the plotting device (see Fig. 3B).

2.2. Micro-fluidic arrangement

The glass cuvette with dimensions $25\ \text{mm} \times 15\ \text{mm} \times 1\ \text{mm}$ bears photolithographically prepared micro-channels having a depth of about $60\ \mu\text{m}$ (Fig. 4) through which the analyte liquid is loaded for interaction with the spot array. In the presence of the analyte liquid the polymer surface of the chip is swollen. The sharp edges of the micro-channels which are in direct contact

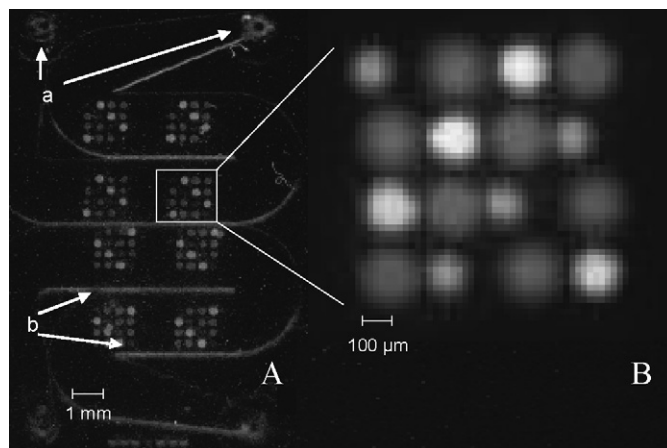


Fig. 4. (A) Dyed micro-spot array inside glass cuvette micro-channel: (a) inlet and outlet apertures and (b) glass cuvette with micro-channel edges. (B) Selected array for CCD imaging.

with the swollen polymer surface concurrently act as a gasket to seal the fluidic channels. This compact liquid interaction micro-chamber (IMC) assembly is the space for the analyte liquid and micro-spot array to come in contact with inlet and outlet apertures. The particular curved nature of the micro-channels provides minimum dead volume of the analyte liquid in the cuvette, facilitating homogeneous fluidic conditions inside the IMC. Also online liquid characterization is possible if the micro-reaction assembly is fitted in series with the inlet of the IMC replacing the auto-sampler in the miniaturized flow through system (Fig. 5). Analytical experiments were carried out with this micro-fluidic set-up integrated in an optical bench, which mainly included the syringe pumps, an auto sampler and the IMC. The auto-sampler sample loop was filled with the analyte liquid and connected to the IMC. The syringe pumps on the other end were

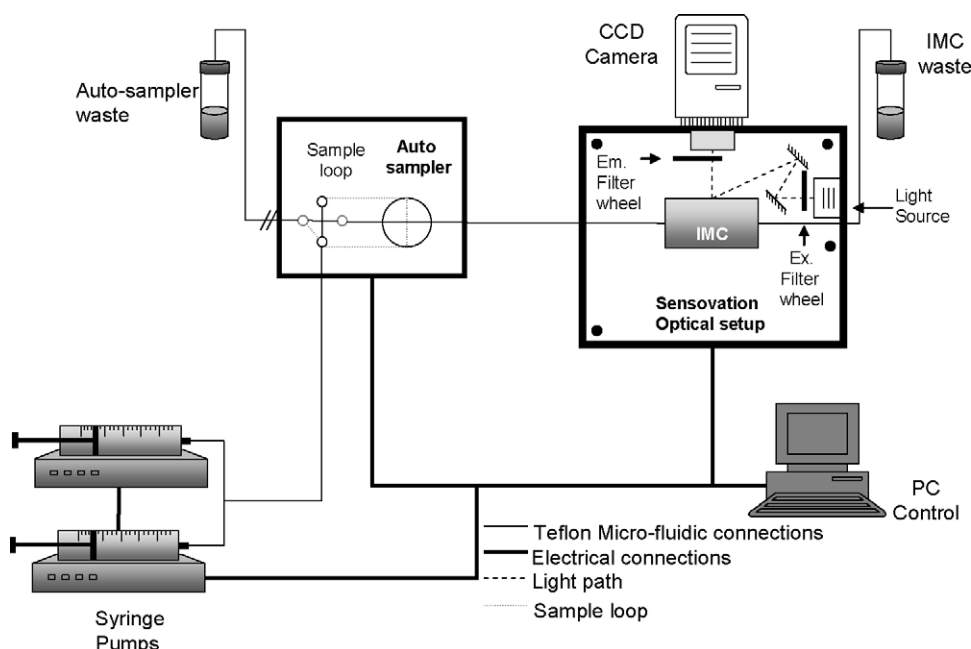


Fig. 5. Optical set-up (Sensovation GmbH) for fluorescence CCD imaging with integrated micro-fluidics.

fitted with syringes containing distilled water or buffer solutions connected to the auto-sampler loop which could push the sample liquid from the auto-sampler loop into the IMC under controlled delivery parameters like flow rate and sample volume. Teflon tubing with 0.5 mm inner diameter was used to connect all fluidic peripherals.

Consequently the IMC can be washed with solvent or distilled water following the analyte liquid. The complete experimental operation was automated and computer controlled using dedicated software based on LabVIEW™ (National Instruments) program package.

2.3. Optical set-up fluorescence imaging

The optical set-up primarily comprises of a CCD camera (CoolSamBa HR-320) with a resolution of 3.2 mega pixels, which creates an image of 2184×1472 pixels with a pixel size of $6.8 \mu\text{m} \times 6.8 \mu\text{m}$. The CCD chip is cooled to about 60°C below room temperature, which provides high efficiency and a good signal to noise ratio. Images are created by the shutter situated next to the light source with controlled exposure and shutter delay timings. A gray scale image with 16-bit resolution was created with an arbitrary gray scale value (GSV) for the pixels, which represents the fluorescence intensity of the area on the chip (array). The integration time of the CCD chip varies from $100 \mu\text{s}$ to 5 s which allows the set-up to be used for dynamic fluid analysis via fast imaging. The IMC can be mounted in front of the camera lens on a slide rule with XYZ fine adjustments for camera focusing. The filter wheels are used to fit the excitation and emission filters. Band pass excitation filters with bandwidth of 30–50 nm were used. Corresponding emission filters with similar bandwidth were fitted on the emission filter wheel. Concave mirrors were positioned to propagate the light beam in order to illuminate the IMC. The beam diameter was 2.5 cm so as to expose almost the whole cuvette facing the camera lens. Camera parameters like exposure time, integration time and the source intensity were adjusted according to the dye fluorescence intensity to fit the upper and lower limits of the fluorescence detection sensitivity of the camera CCD chip. The software 'Image-J' (freeware) was used for image processing. We chose the visually homogeneous area inside the spot for calculating the average GSV of the pixels.

2.4. Measurement procedures

The intensity of the array was equilibrated with distilled water for reference imaging. Syringes mounted on the syringe pumps were filled with distilled water which acted as a carrier liquid. The initial GSV for the fluorescent spots was adjusted to the maximum resolution of 16 bits using camera parameters of exposure time and integration procedures.

The programmed experimental steps began with the stop flow method, capturing images of the IMC under distilled water. The auto-sampler loop was filled with sample analyte liquid. The carrier liquid from syringes pushed the analyte liquid into the IMC and replaced the complete volume inside the IMC with the analyte liquid in a time period of 15 s. The flow rate and volume, for

Table 1

Polarity samples used with E_N^T empirical scale values calculated from the absorption λ_{max} measurements of Reichardt's betaine dye

	DSMO content in water					
	100	90	70	50	30	10
E_N^T scale	0.44	0.59	0.81	0.92	0.96	0.99

Table 2

pH solutions used as analyte probes

	Buffer used					
	Citrate–phosphate	Citrate	Citrate	Phosphate	Phosphate	NaHCO ₃
pH	4.7	5.3	6.0	7.4	8.0	10.0

the feeding of analyte sample into the IMC was standardized. A stabilization time of 1 min was given to allow for homogeneous fluidic conditions inside the IMC. All pictures were also taken in static fluidic conditions, so as to avoid sheer stress on the polymer matrix. The IMC was washed again with the carrier liquid till the GSV returned to its original value. This was in turn the initial value for the next analyte liquid. All standardized experimental steps were programmed in the LabVIEW™ software and were completely automated.

2.5. Test analytes

Dimethyl sulphoxide (DMSO) was diluted with varying amounts of water in order to prepare the analyte sample with different polarities (Table 1). Different standard buffer solutions were prepared and used as pH analyte samples (Table 2).

3. Results and discussion

The digital images recorded with the CCD camera were saved in the TIFF format and analysed for the GSV of the spots. These images had an upper cut off at GSV 6553 and below 3000 were treated as the back ground count with an estimated noise of 100. The absolute GSV count of the dye spot varies with the amount of dye bound to the polymer surface. Each dye spot has its characteristic initial intensity which depends on its intensity at the given excitation wavelength and the overlapping area of its absorption spectrum with a band pass spectrum of the excitation filter.

According to the type of dye used in the construction of the spot array, the initial GSV of the images differ slightly from array to array and spot to spot depending on the reproducibility of the preparation procedure steps of the array.

The problem of signal identification from digital images for optical intensity change is handled by simple arithmetic operations. Generally, the gray scale or color values are added or subtracted to know the change in the optical signal which is always based on the reference picture. Here, we have used a slightly different method in which we compared the percentage change of fluorescence intensity in the GSV of the spots in the array from their initial intensity (before interaction with the

analyte) to the GSV of the spots after analyte interaction. This signal was plotted against the solvent composition (Fig. 7). As mentioned earlier, there might be leaching of dye observed in the case of some analytes. In order to have a better calibrated system we treated the new GSV of the leached spot as the zero value (reference value) and calculated the percentage change in fluorescence intensity from that new value. The array showed a typical pattern of fluorescence alteration with respect to the change in the analyte sample characteristics. A polarity response is represented in Fig. 6. Dye 1 and dye 2 which were typical polarity indicators showed opposite behavior. Spots of dye 1, positioned along the diagonal of the array showed a gradual decrease in fluorescence intensity with the decrease in polarity of the sample analyte. On the other hand the fluorescence intensities from the spots of dye 2 were increased with decreasing analyte sample polarity (Fig. 7a and b). A similar response was also shown by dye 3 and dye 4, but the change in fluorescence intensity was comparatively lower. The extent of fluorescence intensity change between dye spots 1 and 2 is also different. Dye 1, is more sensitive towards change in polarity in comparison with dye 2 and shows a percentage increase in fluorescence intensity of up to 180%. On the other hand the percentage decrease in fluorescence intensity of dye 2 goes down only by about 45%.

The other two (pH indicator) dyes used in micro-arrays were Fluorescein (dye 3) and Rhodamine-B (dye 4) in their salt forms. The sodium salt of Fluorescein makes it an anionic dye, while chlorine salt of Rhodamine-B makes it a cationic dye.

These dyes once again show opposite behavior towards the pH analyte liquids (see Fig. 7c and d). Fluorescein is a pH indicator fluorescent dye which shows a pH-dependent ionic equilibrium also in dianionic form with high fluorescence

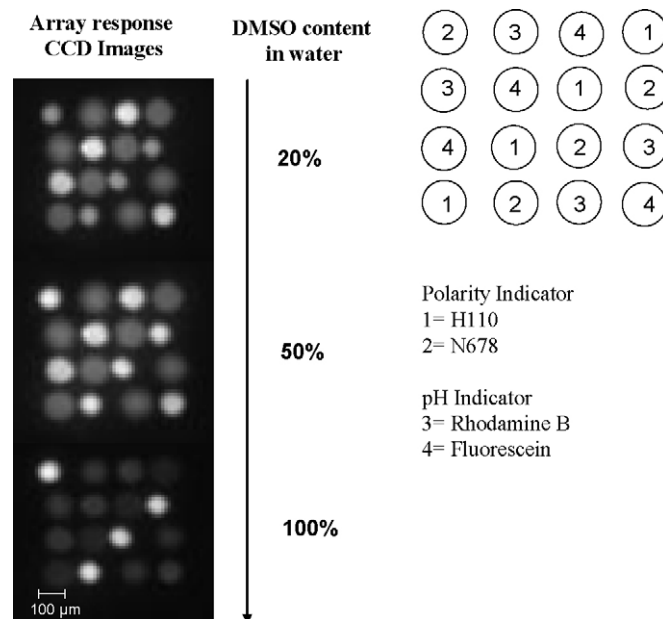


Fig. 6. Optical response of a micro-spot array towards the polarity analyte liquids. Fluorescence intensity of different dye spots changed characteristically as the polarity of the analyte liquid.

intensity. Hence it also shows a considerably larger percentage fluorescence quantum yield change which is up to 95% while with Rhodamine-B the percentage intensity change lowers only by around 22%. These data also emphasized the fact that although the GSV of each individual spot was scattered considerably, the percentage change in the fluorescence intensity of each spot was in good agreement with the exception of dye 1, for lower polarity analyte samples.

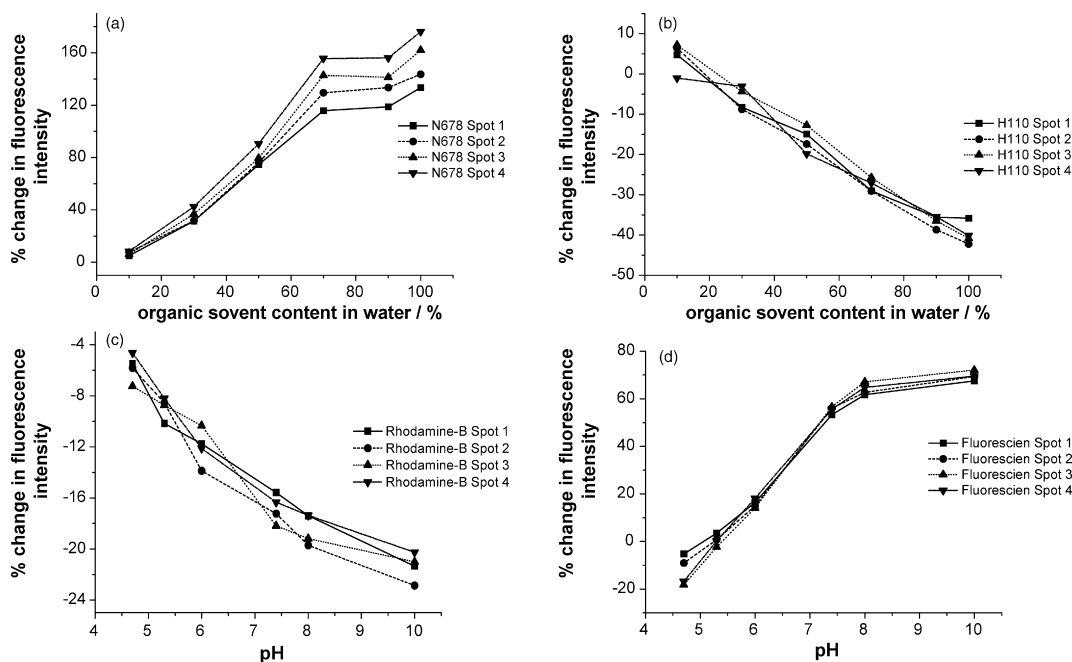


Fig. 7. Reproducibility of the fluorescence signal from different spots of same composition depending on polarity and pH, after spot fluorescence intensities were analysed for percentage change with respect to reference intensity in the solvent (distilled water). (a and b) Percentage fluorescence intensity change of the polarity indicator dyes spots. (c and d) Percentage intensity change of pH indicator dye spots.

4. Conclusion and outlook

The sensitive technique of fluorescence change detection was applied in array technology for the successful identification and characterization of solvent mixtures by measuring the polarity and pH of various analyte samples. The commercially available dyes were effectively used for the micro-array construction and analyte sample characterization by adopting an empirical approach. The non-specific interaction approach widens the span of application of the chemo-chips in the field of chemical sensors. This work sets the foundation for the enlarged array, with more identification functions as probes. The fundamental power of this chemo-chip approach using fluorescence micro-spot arrays consists in its applicability to biological analytes or more complex liquids due to its high sensitivity and unique response for each different analyte. Future work will focus on the advancement of the array size, composition of the single spot in the array, its contents and identification properties. Standardization of a fluorescence pattern from such an array for the response to the analyte–array interaction can be done to create the optical fingerprinting criterion for identification and characterization of common chemical analyte liquids and complex composed liquids like common beverages.

Acknowledgements

The present work was a part of the ‘Chemo-Chips’ project and funded by the VDI-VDE Innonet project. The authors thank the project coordinator Prof. Feller for his important support. The technical support by Steffen Schneider and Jens Albert is gratefully acknowledged.

References

- [1] B. Lemieux, A. Aharoni, M. Schena, *Mol. Breed.* 4 (1998) 277.
- [2] A. Benko, M. Prince, B.J. Price, N.T. Kaltcheva, P. Geissinger, A.W. Schwabacher, *J. Combinatorial Chem.* 8 (2006) 221.

- [3] H.C. Tsai, R.A. Doong, *Biosens. Bioelectron.* 20 (2005) 1796.
- [4] Z.H. Liu, S.Y. Gao, T.L. Chen, *J. Polym. Sci. Part a: Polym. Chem.* 43 (2005) 3447.
- [5] M. Cajlakovic, A. Lobnik, T. Werner, *Anal. Chim. Acta* 455 (2002) 207.
- [6] G.E. Badini, K.T.V. Grattan, A.C.C. Tseung, *Analyst* 120 (1995) 1025.
- [7] W.H. Steel, Y.Y. Lau, C.L. Beildeck, R.A. Walker, *J. Phys. Chem. B* 108 (2004) 13370.
- [8] R.A. Walker, C.L. Beildeck, W.H. Steel, *Abstr. Pap. Am. Chem. Soc.* 228 (2004) U213.
- [9] W.H. Steel, C.L. Beildeck, R.A. Walker, *J. Phys. Chem. B* 108 (2004) 16107.
- [10] G. Ambrosi, P. Dapporto, M. Formica, V. Fusi, L. Giorgi, A. Guerri, M. Micheloni, P. Paoli, R. Pontellini, P. Rossi, *Chem. Eur. J.* 9 (2003) 800.
- [11] I.J. Shin, J.W. Cho, D.W. Boo, *Combinatorial Chem. High Throughput Screen.* 7 (2004) 565.
- [12] H.D. Inerowicz, S. Howell, F.E. Regnier, R. Reifengerger, *Langmuir* 18 (2002) 5263.
- [13] C. Zhang, K.S. Suslick, *J. Am. Chem. Soc.* 127 (2005) 11548.
- [14] D. James, S.M. Scott, Z. Ali, W.T. O’Hare, *Microchim. Acta* 149 (2005) 1.
- [15] K.S. Suslick, N.A. Rakow, A. Sen, *Tetrahedron* 60 (2004) 11133.
- [16] K.J. Albert, N.S. Lewis, C.L. Schauer, G.A. Sotzing, S.E. Stitzel, T.P. Vaid, D.R. Walt, *Chem. Rev.* 100 (2000) 2595.
- [17] J.P. Santos, J. Lozano, A. Aleixandre, I. Sayago, M.J. Fernandez, L. Ares, J. Gutierrez, M.C. Horrillo, *Sens. Actuators B-Chem.* 103 (2004) 98.
- [18] P. Ciosek, Z. Brzozka, W. Wroblewski, *Sens. Actuators B-Chem.* 103 (2004) 76.
- [19] S. Ehrmann, J. Jungst, J. Goschnick, D. Everhard, *Sens. Actuators B-Chem.* 65 (2000) 247.
- [20] J.W. Gardner, T.C. Pearce, S. Friel, P.N. Bartlett, N. Blair, *Sens. Actuators B-Chem.* 18 (1994) 240.
- [21] J.W. Gardner, H.V. Shurmer, T.T. Tan, *Sens. Actuators B-Chem.* 6 (1992) 71.
- [22] M.C. Janzen, J.B. Ponder, D.P. Bailey, C.K. Ingison, K.S. Suslick, *Anal. Chem.* 78 (2006) 3591.
- [23] C. Bohne, H. Ihmels, M. Waidelich, Y.W. Chang, *J. Am. Chem. Soc.* 127 (2005) 17158.
- [24] L. Dasilva, C. Machado, M.C. Rezende, *J. Chem. Soc.-Perkin Trans. 2* (1995) 483.
- [25] C. Reichardt, *Solvent and Solvent Effects in Organic Chemistry*, VCH, 1990.